# INSIGHT

"ImplementatioN in real SOFC Systems of monItoring and diaGnostic tools using signal analysis to increase tHeir lifeTime"

Grant Agreement n° 735918 –
Research and Innovation Project

Deliverable D2.5.
Faults/failures implemented on SRU/SS/Stack and EIS/THD techniques as a detection tool
Deliverable D2.6.
Lifetime tests performed on SRU/SS/Stack and EIS/THD techniques as a diagnostic tool
Final report

**Start date of the project:** 1st January 2017
**Duration:** 36 months
**Project Coordinator:** Julie MOUGIN – CEA

**Contact:** Julie MOUGIN – CEA LITEN France - julie.mougin@cea.fr

## Document Classification

| | |
|---|---|
| **Title** | ***Faults/failures implemented on SRU/SS/Stack and EIS/THD techniques as a detection tool – final report***<br><br>***Lifetime tests performed on SRU/SS/Stack and EIS/THD techniques as a diagnostic tool – final report*** |
| **Deliverable** | D2.5. and D2.6 |
| **Reporting Period:** | P2 |
| **Date of Delivery foreseen** | M30 |
| **Draft delivery date** | 02/10/2019 |
| **Validation date** | 29/02/2020 |

| | |
|---|---|
| **Authors** | A. Ploner (DTU), A.Hagen (DTU), H. Moussaoui (EPFL), S. Pofahl (AVL), G. Nusev (IJS), P. Boskoski (IJS), B. Morel (CEA) |
| **Work package** | WP2 Experimental testing and Calibration |
| **Dissemination** | **PU** |
| **Nature** | **R** |
| **Version** | *V1* |
| **Doc ID Code** | |
| **Keywords** | Testing, EIS, THD, PRBS, DRT, faults; lifetime test, diagnostic |

## Document Validation

| Partner | Approval (Signature or e-mail reference) |
|---|---|
| **P1 - CEA** | e-mail |
| **P2 - DTU** | |
| **P3 - UNISA** | |
| **P4 - EPFL** | |
| **P5 - JSI** | |
| **P6 - VTT** | |
| **P7 - AVL** | |
| **P8 –SP** | |
| **P9 - HTc** | |
| **P10 – BIT** | |
| **P11 – AK** | |

**This project has received funding from the Fuel Cells and Hydrogen 2 Joint Undertaking under grant agreement No 735918. This Joint Undertaking receives support from the European Union's Horizon 2020 research and innovation programme, Hydrogen Europe and Hydrogen Europe research.**

## Document Abstract

The aim of this document is to present the results of the tests performed during the second period in the frame of WP2. It is a follow-up of deliverables D2.3 and D2.4 delivered in M18 and covers both short stacks and large stack. This document merges D2.5 and D2.6 to evaluate EIS/THD techniques as both diagnostic and detection tools.

Tests have been performed at DTU, EPFL and CEA according to test protocols and specifications defined in D2.1 with a focus on 3 faults/failure: fuel starvation, carbon deposition and gas leakage. EIS (Electrochemical Impedance Spectroscopy) associated to DRT (Distribution of Relaxation Times) analysis, THD (Total Harmonic Distortion) and PRBS (Pseudo-Random Binary Signals) measurements as well as conventional signals have been considered and their potential as detection and diagnostic tools has been evaluated.
AVL and IJS have installed their specific devices respectively at EPFL and CEA to be used for measurements during the tests.

For the testing campaign presented in the present report, carbon deposition and gas leakage are considered for short stack testing campaign.
Finally, a 32-cell stackbox has been tested, with the fuel starvation protocol.

*Carbon deposition:*
Two different experiments were conducted and EIS on the single repeat unit (RU) and stack level were implemented to detect flawed operating conditions, which could cause detrimental failure by locally introduced carbon formation. Generally, it could be observed that in both simulated cases, these changes led to increase in cell voltage which seems to be a good metric extractable solely from the stack voltage. Furthermore, the complimentary use of EIS measurements/metrics on stack level allow detection of the condition changes. In the first case (=SC ratio reduction), an increase of high frequency area specific resistance in parallel with a decrease of the low frequency arc indicates possible critical conditions. In the second case, again an increase of the high frequency circle, together with an increase of the low frequency arc can be used as a detection metric for unsafe conditions. Yet both simulated failures, did not give any indication of a final detrimental failure occurring inside the stack.

*Gas leakage*
A gap sealing close to the outlet of the stack cannot be easily detected from open circuit voltage (OCV) nor IV characterizations. A specific protocol based on OCV measurements at different air and fuel flowrates seems to give meaningful results.
The defect “gap in the sealing close to the stack inlet” can be more easily detected than a gap located close to the outlet of the stack. It can most clearly be observed in the OCV. At the RU level its signature is related to the increase in steam content, which results in a reduction of the polarization resistance as measured by EIS. DRT analysis reveals that it is the gas conversion peak (P2) that is reduced, whereas peak P3, which is attributed to gas diffusion in the porous anode structure, is shifted towards higher frequencies. However, at the cluster level, this signature cannot be detected anymore due to averaging with defect-free RUs.

*Stackbox test*
On the 32-cells Stackbox, PRBS and sine excitations are recorded properly and automatically every 3 h during the fuel starvation protocol where the fuel utilization FU is increased from 0.8 to 0.875. A detailed analysis is needed to extract useful information and metrics from these data and to see if we are able to detect the signature of fuel starvation at the cluster level despite the averaging effect.

*Use of classical signals*

Classical signals remain a useful tool to see a deviation of a stack/system from its standard operating conditions. It was particularly useful for the case of a leakage, in association with some specific deviation trials as compared to the nominal operating conditions to highlight the issue.

*Electrochemical Impedance Spectroscopy (EIS)*

EIS was found to be an adequate technique to identify the carbon deposition fault, at stack level. On the contrary, for gas leakage, it was found to be efficient at the RU scale, and DRT analysis further allowed to identify the frequency signature of the defect. However, on the clusters level (6-cell short stack), the signature of the defect was unfortunately lost through averaging.

*Pseudo-Random Binary Signals (PRBS)*

EIS diagrams extracted from PRBS excitation are well superimposed to those obtained from sines excitation, meaning that PRBS is a valuable technique in order to obtain faster EIS results that do not disturb too long the stack/system from its setpoint during real operation.

*Total Harmonic Distortion (THD)*

The THDA method is sensitive to higher FU even far away from the critical region above FU = 75%, the method is therefore a suitable indicator to enhance system reliability combined with higher efficiency.

## Table of Contents

## 1. Introduction

In INSIGHT project, WP2 focusses on experimental tests at Single Repeat Unit (SRU) and Short Stacks (SS) to characterize them when operated with faults. The tests follow the protocols defined in D2.1 and concentrate on three types of faults considered as the most meaningful in D2.2 following the following criteria: the severity and frequency of the degradation phenomena, their detectability, and the potential for mitigation or recovery measures. Those faults are fuel starvation, carbon deposition and gas leakage.
The protocol defined in D2.1 consider routine durability tests, and the on-purpose introduction of the aforementioned faults. Therefore, different modules are suggested which can be combined individually. Two durability modules and different fault modules are suggested. Each test program follows a standardized sequence consisting of: start-up and initial characterization, the actual durability period, and a final characterization. The durability modules contain the most important degradation initiating set of conditions, starting with baseline operation at constant conditions, followed by the introduction of the fault incidents.
It can be seen from the description above that faults and lifetime tests are very imbricated, as well as the question of detection and diagnostic tool. For that reason and as for D2.3 and D2.4 which were merged, the present deliverable is a joint one, so-called D2.5&D2.6. It presents the experimental results obtained by the different testing partners involved in WT2.3 and sharing the testing matrix: DTU, EPFL, CEA. Partners involved in detection and diagnostic measurements such as AVL and IJS also contributed in the measurements presented in the present deliverable thanks to the installation of their specific devices respectively at EPFL and CEA to be used for measurements during the tests. All tests were performed on SOLIDpower 6-cell short stacks modified or not and on a 32-cells Stackbox.
For the testing campaign presented in this final report, fuel starvation, gas leakage and carbon deposition are considered. Fuel starvation has been considered either by decreasing the overall fuel flow while keeping the current density constant or by increasing the current density while maintaining the flow. Gas leakage has been considered either by the introduction of a leakage in the sealant, on fuel inlet or outlet. Carbon deposition protocol has been performed in this second testing campaign.
EIS (Electrochemical Impedance Spectroscopy) associated to DRT (Distribution of Relaxation Times) analysis, THD (Total Harmonic Distortion) and PRBS (Pseudo-Random Binary Signals) measurements in addition to conventional signals are considered and their potential as detection and diagnostic tools is evaluated.

## 2. Tests performed at DTU

### 2.1. Description of the tests

Carbon deposition and leakage detection measurements were conducted on a 6-cell short stack delivered by Solid Power Italy. The pre-reduced stack was heated up to the operating temperature of 750°C (reference temperature = air outlet temperature) at a constant flow of $H_2$:$N_2$ 9:91 and air. After this procedure, EIS and iV investigation on the stack were performed in $H_2$ and $CH_4$ gas compositions with air as oxidant.

**Leakage** For the leakage test, a gap in the sealing was deliberately introduced at repeating unit (RU) 4 of the 6-cell stack. Conventional signals (i.e. temperature, stack voltage) were recorded during OCV and at operating conditions in order to detect the fault.

**Carbon deposition I** The carbon deposition fault was simulated by decreasing the steam-to-carbon ratio via reduction of the steam content in the used $CH_4$:$H_2O$ fuel while keeping the $CH_4$ flow

constant. The stack was operated galvanostatically at a current density = 0.4 A $cm^{-2}$ with an initial SC ratio of 2. The ratio was thereafter stepwise decreased (i.e. SC=2 – 1.5 – 1 – 0.5) and at each operating condition conventional signals and EIS were monitored for at least 24 h. For the last 24 h of the 'carbon deposition fault' simulation, the stack was set back to initial operating conditions.

**Carbon deposition II** After extraction of relevant signals/metrics in the carbon deposition I experiment, a second experiment was conducted by decreasing the current density during operation. The stack was therefore initially operated at a current density of 0.3 A $cm^{-2}$ with a 1:1 $CH_4$:$H_2O$ ratio, followed by monitoring for at least 24 h at 0.2 – 0.1 – 0.05 – 0 A $cm^{-2}$. For the final 24 h of the test, the stack was set to 0.2 A $cm^{-2}$ for recovery.

## 2.2. Faults/failure implemented

### 2.2.1. Results

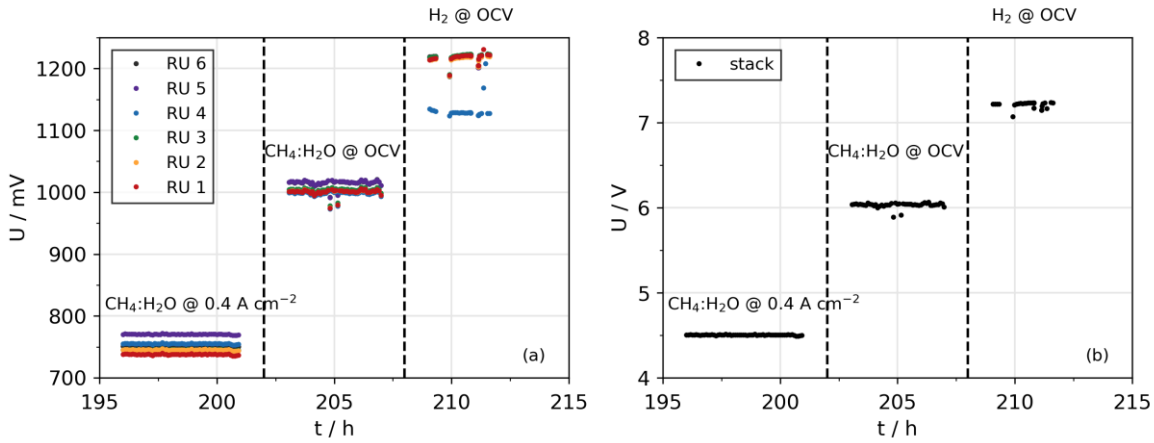


Fig. 1. Cell voltages of each RU (a) and stack voltage (b) at 0.4 A $cm^{-2}$ operated with $CH_4$:$H_2O$ 1:2 fuel (first segment), at OCV with the same fuel gas composition (second segment) and at OCV with dry $H_2$ fuel (third segment). For better visualization polarization measurements at each steps are excluded.

**Leakage - Fault detection via 'conventional signals'.** Fig. **1** shows the stack voltage and the individual cell voltages of RU 1-6 under operation (j = 0.4 A $cm^{-2}$, $CH_4$:$H_2O$ 1:2, FU 77%), at OCV conditions in $CH_4$:$H_2O$ 1:2 fuel and dry $H_2$ fuel. The cell voltage of RU4 clearly stays approx. 100 mV below the remaining RUs in the last segment (dry $H_2$). In contrast, the stack voltage signal alone in dry $H_2$ or operation under current and introduction of steam ($CH_4$:$H_2O$ fuel) doesn't allow distinguishing the leaky element. Therefore, the leakage fault only becomes obvious under dry fuel conditions at OCV and detection requires monitoring of individual cell voltages.

**Carbon deposition I - Fault detection via 'conventional signals'.** In Fig. **2** the voltage recording of each RU (a) and the total stack voltage (b) vs. time are displayed. The successive steam content reduction resulted in a nearly constant increase of the cell voltage between 15 – 20 mV per RU per step, whereas increasing the steam feed in the final sequence caused the cell voltage to level out close to the initial cell voltage at the beginning of the test. The observed operation signals are therefore suggesting non-detrimental operating conditions.
The noticeable fluctuations of the voltage signal are a result of the electrochemical impedance measurement at the initial and final part of each step. However, the nearly periodically fluctuations recorded at the SC ratio = 0.5 are most likely caused by an instability of the installed fuel gas pre-

heater in the testing station. With the change in gas compositions the fuel gas pre-heater temperature successively increased in a likewise manner. After trespassing an apparent threshold of ca. 400 ºC these fluctuations could be seen in the cell voltage recording. However, at this stage, the occurring phenomenon is not yet understood and requires further investigation, but it could be caused by locally occurring carbon deposition in the pre-heater.

Additionally temperature measurement of in- and outlet fuel gas and air were recorded (not shown here); however the monitored changes varied only by 2-3 degrees during the 'step-experiment' and therefore didn't allow identifying any obvious malfunction.

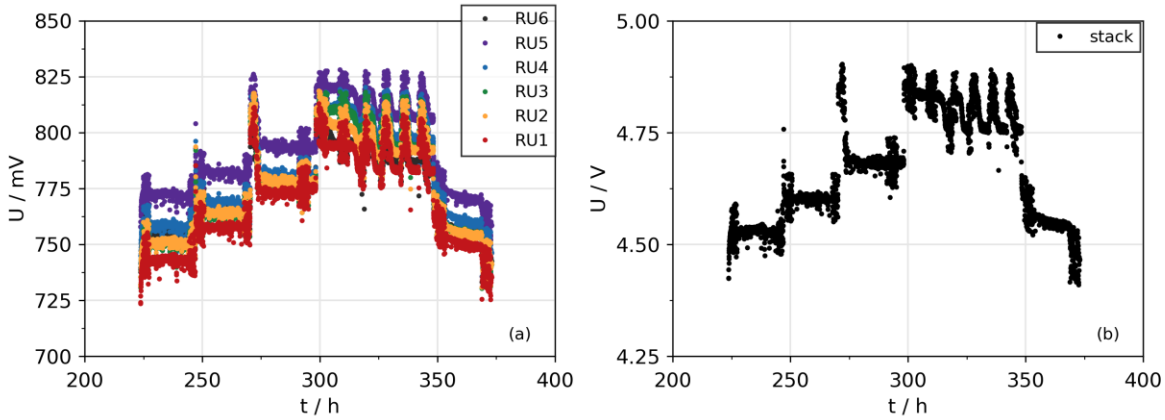


Fig. 2. Cell voltages of each RU (a) and stack voltage (b) monitored while decreasing the SC-ratio from 2 to 0.5 at 0.4 A $cm^{-2}$. For the final 24 h of the test, the stack was set back to the initial testing conditions.

**Fault detection via EIS.**

Aside from voltage and temperature measurements, EIS was performed. Recorded Impedance Spectra (IS) at each SC reduction step are presented in Fig. **3**. The averaged RU IS (i.e. recorded stack IS/number of RU) and of the first RU1 show similar trends. With each decrease in steam feed, an increase of the semi-circle in the high frequency region occurs and is accompanied by an opposite

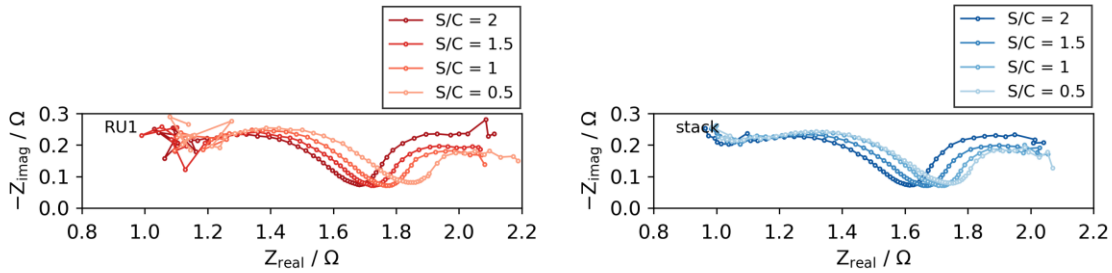


Fig. 3. IS of RU1 (left) and of the averaged RU from stack IS (right) at different SC ratio. The SC ratio was caused by decreasing the steam feed in the fuel. Please note that presented EIS data is including artefacts of the testing station. Nevertheless, the EIS data allowed fault metric identification.

trend of the low frequency region arc. Regarding the serial resistance, no or only minimal changes are detected.
These changes clearly reflect the fuel gas composition changes varied at each step, yet the '0.5 SC-ratio step' (also recorded over time) did not change considerably and no carbon formation became apparent. Yet, the observed IS pattern can be used as a preliminary fault signal, indicating an atypical gas composition. Moreover, recording of solely the stack impedance enables detection.

**Carbon deposition II - Fault detection via 'conventional signals'.** After no obvious detrimental issue/fault was detected while conducting the 'carbon deposition I' experiment', another fault investigation experiment on the same stack was performed. In Fig. **4** measurements of cell voltages of each RU and stack at different current densities in a $CH_4$:$H_2O$ 1:1 fuel are presented. Likewise to the carbon deposition I experiment, a decrease in operating current caused an increase in cell voltage. For the explanatory chosen RU1 each 0.1 A $cm^{-2}$ step caused a voltage increase of approx. 66 to 79 to 85 mV – indicating a non linear increase of cell voltage current dependency. Similar to the fluctuation discussed in the 'carbon deposition I' experiment, the pre-heater influence can also be seen here. After identifying this correlation, the pre-heater temperature was deliberately reduced below 400°C and therefore the fluctuations are not occurring in the last two steps.
Aside from this phenomenon, no evident sign of a detrimental stack malfunction could be detected while conducting the experiment. The last 'recovery step' reached again the initial cell voltage at 0.2 A $cm^{-2}$.

The simultaneously performed temperature monitoring of the fuel and oxidant gas at the stack in- and outlet gas decreased in parallel to each 'current density decreasing step'. In total the temperature reduced by approx. 8°C. This reflects primarily the decreasing influence of the joule heating effect.

**Fault detection via EIS.** Each step was furthermore monitored by EIS over time. The resulting IS at each 'current-reduction step' are given in Fig. **5**. Primarily, the resistance of the semi-circle at high frequencies shows a stepwise increase with a co-occurring slide increase of the low-frequency semi-

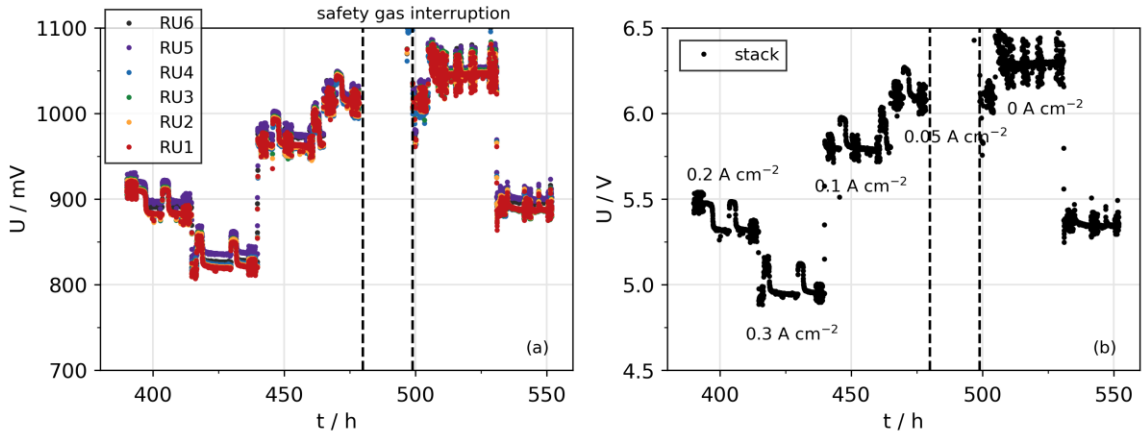


Fig. 4. Cell voltages of each RU (a) and stack voltage (b) monitored while decreasing the current density from 0.3 to 0 A $cm^{-2}$ at SC=1. For the final 24 h of the test, the stack was set to j=0.2 A $cm^{-2}$. An interruption of the test at 480-499 h was caused due to a precaution system of the testing station, setting the stack to OCV in forming gas.

circle. Yet, at OCV('zero-current step') the low-frequency arc expands tremendously, thus being an obvious metric for reaching the most critical conditions.
In summary however, EIS over time at each step did not indicate any significant change, so no sign for any destructive stack/cell failure could be extracted. The IS metric are therefore only monitoring the change of conditions, showing that the stack is now operating under unsafe conditions. Similarly to the carbon deposition I experiment, the metrics can be extracted solely from a stack impedance measurement and do not necessitate the implementation of single RU measurements.

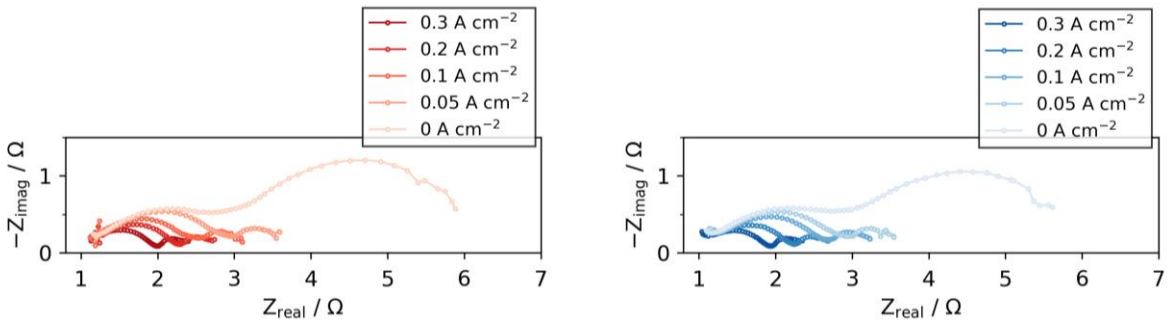


Fig. 5. IS of RU1 (left) and of the averaged RU from stack IS (right) at different current densities. Please note that presented EIS data is including artefacts of the testing station. A testing station impedance will be recorded to subtract and account for the testing station impedance. Nevertheless, the EIS data allowed fault metric identification.

### 2.2.2. Conclusions on EIS/THD techniques as a detection tool

Two different experiments were conducted and EIS on the single RU and stack level were implemented to detect flawed operating conditions, which could cause detrimental failure by locally introduced carbon formation. Starting with the nominal operation conditions at 0.4 A $cm^{-2}$ in $CH_4$:$H_2O$ 1:2 at 77% FU, two scenarios were investigated: Firstly, a reduction of the steam feed in the fuel gas was considered to simulate a realistic malfunction during operation. This can lead to a

critical SC ratio where carbon deposition might only locally occur. Secondly, at low SC operation a failure of the power electronics may cause conditions, where the intrinsically – during operation – generated steam is reduced to a level at which the thermodynamic limits for carbon formation (SC ratio and temperature) are met.
Generally, it could be observed that in both simulated cases, these changes led to increase in cell voltage which seems to be a good metric extractable solely from the stack voltage. Furthermore, the complimentary use of EIS measurements/metrics on stack level allow detection of the condition changes. In the first case (=SC ratio reduction), an increase of high frequency area specific resistance in parallel with a decrease of the low frequency arc indicates possible critical conditions. In the second case, again an increase of the high frequency circle, together with an increase of the low frequency arc can be used as a detection metric for unsafe conditions. Yet both simulated failures, did not give any indication of a final detrimental failure occurring inside the stack.

## 3. Tests performed at EPFL

### 3.1. Description of the tests

In complementary to the leakage detection analysis reported in D2.3-D2.4, the influence of the sealing gap position was investigated in this work. In this objective, the same 6-cell SOLIDpower Short-Stack (SS) was considered but the sealing gap was moved from the cell outlet to the inlet. The gap diameter was kept at 3mm and the same testing protocol was adopted.

### 3.2. Faults/failure implemented

#### 3.2.1. Results

First, the individual RU voltage evolution has been acquired for each of the six cells (cf. Fig 6). There is nothing particular to report except that all voltages stabilized around 1.1 V, which is lower than what was reported for the other short-stacks. Only RU5 is higher than the rest, with 1.18 V. The lowest OCV is that of RU4, but the differences remain slight.

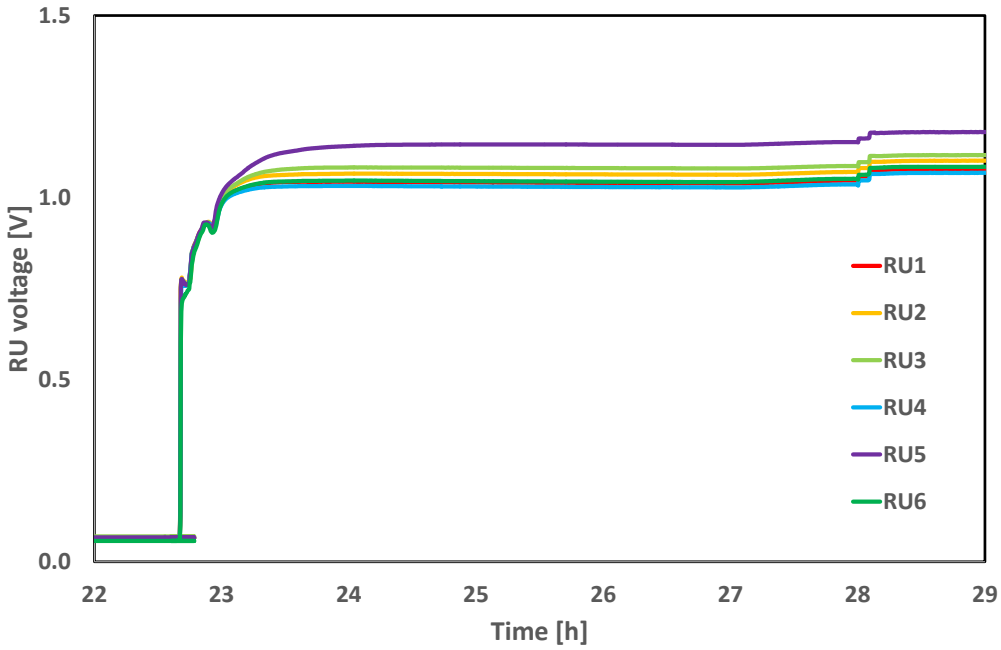


Fig. 6. Evolution of RU voltages during reduction.

The initial *i-U* characterization is shown in Fig. 7. As stated above, RU4 has the lowest OCV but under polarisation it is RU6 that shows the lowest voltage at 0.4 A.cm$^{-2}$. As RU6 is the top RU located the furthest from the fuel inlet, it is expected that this RU sees less fuel in case of leakage in the stack and would therefor experience fuel shortage at high fuel utilization. However, RU5, which is the direct neighbour of RU4, shows the best performance. This strange behaviour could be explained by the fact that the leakage in RU4 produces locally extra steam that increases the pressure drop in the RU4, which results in a redistribution of part of the fuel among the neighbouring RUs 3 and 5. The *i-U* characteristic is quite different from that of the previous case, where the leakage was located close to the outlet. The leakage close to the inlet impacts more severely the OCV of not only the defective RU but also of the neighbouring RUs, indicating that it can more easily be identified during the qualification test of the full stack.

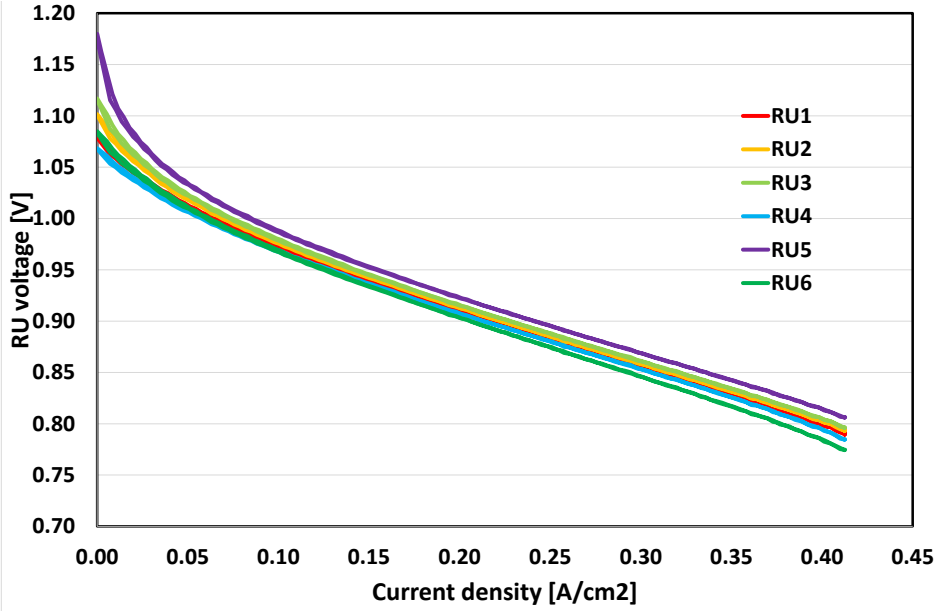


Fig. 7. *i-U* characterization of 6RU short stack with a defective sealing at the inlet in RU4 (conditions: 750°C, air: 32 NL/min).

Fig. 8. shows the EIS spectra as Nyquist plots for both the individual RUs (top) and 3RU clusters (bottom). As the EIS measurement was performed at low current density bias (0.0625A/cm$^2$), the defective RU (RU4) has a smaller polarization resistance due to a higher steam content resulting from the leakage. As for the *i-U* measurement, the defective element can clearly be identified at the single RU level contrarily to the case where the defective sealing is located close to the outlet. However, at the cluster level, this information is lost through averaging. This can be clearly seen in Fig.8 (bottom) by comparing clusters RU1-3 and RU4-6.

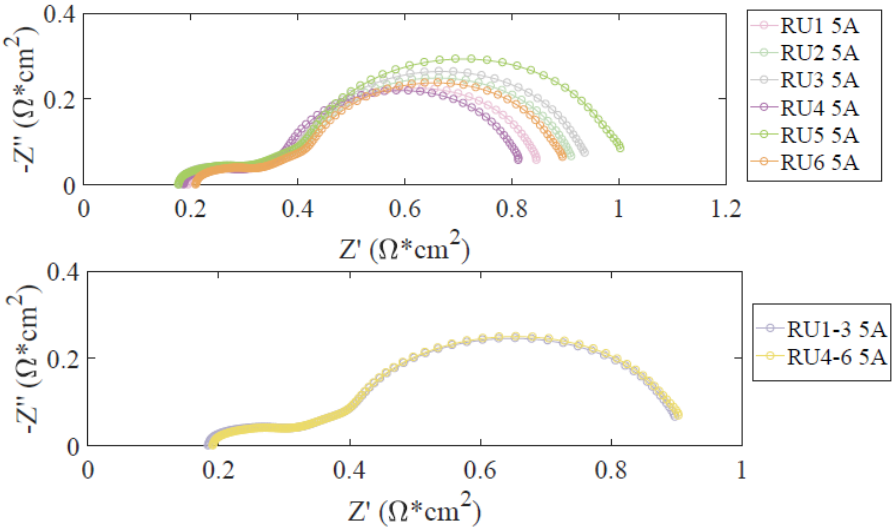


Fig. 8. Nyquist plot of the EIS data measured on a 6-RU short-stack with a defective sealing at the inlet of RU4: (top) individual RU; (bottom) clusters 1-3 and 4-6.

The EIS data was further analyzed by performing DRT. The results are shown in Fig. 9.

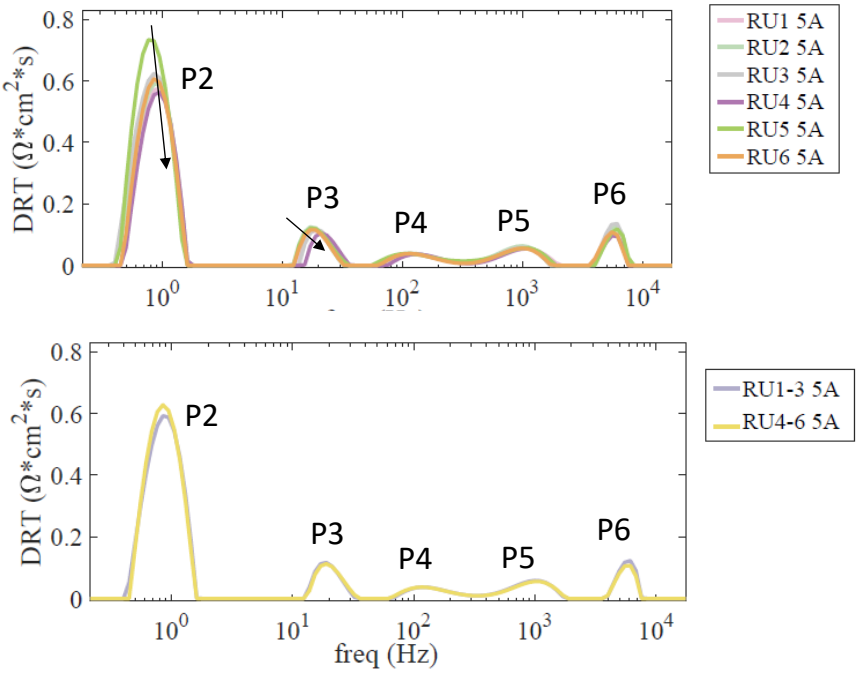


Fig. 9. DRT of the EIS data shown in Fig. 8.

In line with the observation made for Fig. 8, it appears that it is peak P2 that contributes most to the reduction of the polarization resistance of R4 under these operating conditions. As mentioned above, this relates to the steam content which reduces the conversion impedance. Peak P3 is also affected by a shift towards higher frequencies. Nevertheless, this information is lost through averaging, even in the case of 3 RUs.

### 3.2.2. Conclusions on EIS/THD techniques as a detection tool

The defect “gap in the sealing close to the stack inlet” can be more easily detected than a gap located close to the outlet of the stack. It can most clearly be observed in the OCV. At the RU level its

signature is related to the increase in steam content, which results in a reduction of the polarization resistance as measured by EIS. DRT analysis reveals that it is the gas conversion peak (P2) that is reduced, whereas peak P3, which is attributed to gas diffusion in the porous anode structure, is shifted towards higher frequencies. However, at the cluster level, this signature cannot be detected anymore due to averaging with defect-free RUs.

## 4. Tests performed at CEA

### 4.1. Description of the tests

Two tests have been performed during this second period: (1) 6-cells short stack with a sealing defect, (2) 32-cells Stackbox.
The 6-cells short stack with a sealing defect is a stack where a gap (diameter of 3 mm) in the sealing glass has been implemented in the Repeat Unit #3 (RU3) near the outlet of the fuel.

### 4.2. Faults/failure implemented

#### 4.2.1. Results

*Test of the 6-cells short stack with a sealing defect:*

From OCV measurements (see Table 1) under nominal operating conditions (750°C, $H_2/N_2$=3.6/2.4 NmL/min/cm², air=66.7 NmL/min/cm²), we can classify RUs as follow: OCV1=OCV2=OCV4>OCV3>OCV6>OCV5. Hence, RU3 (cell with defect) has not the lowest OCV.

From iV curves under nominal operating conditions (see Fig. 10), the lowest performance is obtained with RU5 (lowest OCV) but it is difficult to say for others RUs.

| U1 | U2 | U3 | U4 | U5 | U6 |
|---|---|---|---|---|---|
| 1.217 | 1.218 | 1.156 | 1.218 | 1.064 | 1.135 |

Table 1. OCV measurements on the 6 RUs (conditions: 750°C, $H_2/N_2$=3.6/2.4 NmL/min/cm², air=66.7 NmL/min/cm²).

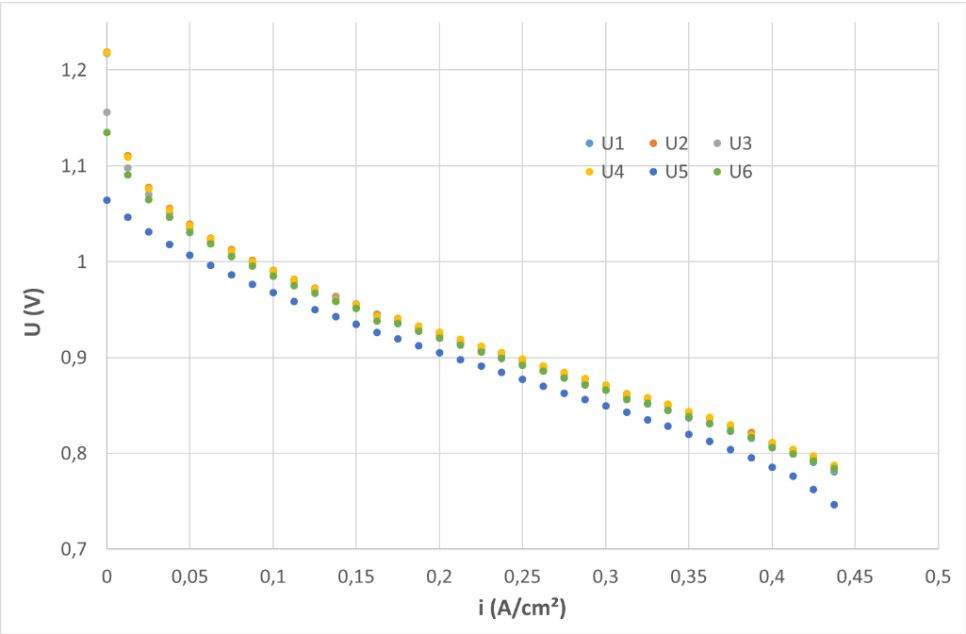


Fig. 10. *i-U* characterization of 6RU short stack with a defective sealing at the outlet in RU3 (conditions: 750°C, $H_2/N_2$=3.6/2.4 NmL/min/cm², air=66.7 NmL/min/cm²).

Sealing leakage close to the outlet flow seems not to have a limiting effect on the stack performance. Because it was not possible to see any impact of the sealing defect using the protocol as defined and the EIS technique, even with DRT analysis, the possibility to perform additional test steps varying some parameters was considered. First the air flow rate was modified, the fuel flow rate being kept constant. Second, both flow rates were kept constant but the $H_2/N_2$ ratio was modified. And finally, the air flow rate was kept constant as well as the $H_2/N_2$ ratio, and the total fuel flow rate was varying. The details are provided in Table 2.

| **Parameter modified** | **Step ref.** | **$H_2$ (Nl/h)** | **$N_2$ (Nl/h)** | **$H_2$ (%)** | **$N_2$ (%)** | **Air (Nl/h)** |
|---|---|---|---|---|---|---|
| Air flow rate varying / Fuel flow rate constant | Step 0 | 103.7 | 69.1 | 0.6 | 0.4 | 1920 |
| | Step 1a | 103.7 | 69.1 | 0.6 | 0.4 | 1440 |
| | Step 1b | 103.7 | 69.1 | 0.6 | 0.4 | 960 |
| Air flow rate constant / $H_2/N_2$ ratio varying, total fuel flow rate constant | Step 0 | 103.7 | 69.1 | 0.6 | 0.4 | 1920 |
| | Step 2a | 69.1 | 103.7 | 0.4 | 0.6 | 1920 |
| | Step 2b | 34.6 | 138.2 | 0.2 | 0.8 | 1920 |
| Air flow rate constant / $H_2/N_2$ constant, total fuel flow rate varying | Step 0 | 103.7 | 69.1 | 0.6 | 0.4 | 1920 |
| | Step 3 | 51.8 | 34.6 | 0.6 | 0.4 | 1920 |
| | Step 0 | 103.7 | 69.1 | 0.6 | 0.4 | 1920 |

Table 2. Detail of parameters modified during the test of the short stack with a sealing leakage issue on fuel outlet of RU3.

It has been found that when air flow rate decreased, OCV of RU3 increases and OCV of RU5 slightly decreases, other cells are constant. When the $H_2/N_2$ ratio decreases, all OCVs decrease. When total fuel flow rate decreases at $H_2/N_2$ constant, all OCVs decrease. The pressure drop measurements tend to show that OCV of RU3 is clearly affected by pressure drop inside fuel/air side, as can be seen on Figure 11. Therefore it can be concluded that for this type of defect, some deviation trials as compared to the nominal operating conditions might be needed to highlight the issue, and the use of convention signals is meaningful.

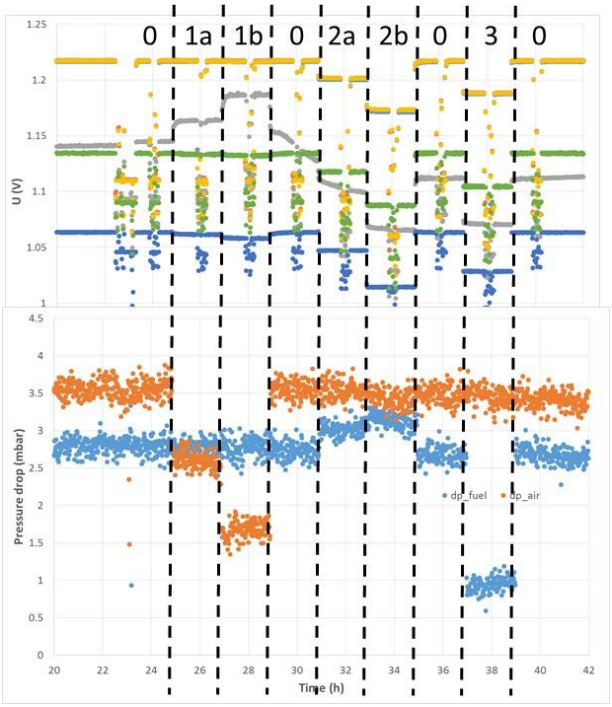


Fig. 11. Evolution of OCV (top) and of pressure drop (bottom) during the testing sequence of Table 2.

*Test of the 32-cells Stackbox:*

The 32-cells Stackbox from SOLIDpower has been installed on a CEA testbench. Modifications of our testbench has implied some delays and the start of the test was effective beginning of 2020.
In particular, there was a need of:
- a air preheater able to preheat the air flowrate of 10 $Nm^3/h$ up to 700°C
- a heat exchanger at the air outlet of the Stackbox able to decrease the temperature of the air outlet below 100°C in order to plug it to the event of our lab.

Figure 12 illustrates the environment of the Stackbox and the table 3 gives the detailed instrumentation implemented on this Stackbox.

(a)

(b)

Fig. 12. (a) SOLIDpower 32-cells Stackbox implemented on CEA testbench and tested in collaboration with IJS. (b) Air preheater of 8 kW able to reach 700°C with an air inlet flowrate of 10 $Nm^3/h$.

| | |
|---|---|
| T_Fuel_Inlet_1 | Temperature of the Fuel Inlet 1 |
| T_Fuel_Inlet_2 | Temperature of the Fuel Inlet 2 |
| T_Fuel_Outlet_1 | Temperature of the Fuel Outlet 1 |
| T_Fuel_Outlet_2 | Temperature of the Fuel Outlet 2 |
| T_Air_Inlet | Temperature of the Air Inlet |
| T_Air_Outlet_1 | Temperature of the Air Outlet 1 |
| T_Air_Outlet_2 | Temperature of the Air Outlet 2 |
| T_Stack_Top | Temperature on the top of the Stack |
| T_Stack_Bottom | Temperature on the bottom of the Stack |
| T_Heating_Cartridge_1 (Safety) | Temperature of the heating cartridge for safety |
| T_Heating_Cartridge_3 (Control) | Temperature of the heating cartridge for control |
| P_Fuel_Inlet | Pressure in the Fuel Inlet (0-30 mbar) |
| P_Fuel_Outlet | Pressure in the Fuel Outlet (0-30 mbar) |
| P_Air_Inlet | Pressure in the Air Inlet (0-30 mbar) |
| P_Air_Outlet | Pressure in the Air Outlet (0-30 mbar) |
| Ui 1≤i≤8 | Voltage (V) of the cluster i, each cluster is composed of 4 cells |

Table 3. Instrumentation on the SOLIDpower 32-cells Stackbox.

From OCV measurements (see Table 4) under nominal operating conditions (750°C, $H_2/N_2$=3.6/2.4 NmL/min/cm², air=66.7 NmL/min/cm²), we can see that all clusters are very close except Cluster1 with more than 10 mV less. We can classify clusters as follow: Cluster5>Cluster2,3>Cluster4>Cluster6>Cluster7>Cluster8>Cluster1.

I-V curve has been measured on the stackbox. Figure 13a represents the stack voltage and the stack power as a function of current density. Figure 13b represents the electrical efficiency as a function of the current density and figure 13c the voltage of the 8 clusters during i-V characterization. At i=33 A (0.413 A/cm²), a fuel utilization FU=0.8, a power P=848 W and an electrical efficiency η=51,3% are achieved. These values are close to those achieved by SOLIDpower before the delivery of the Stackbox. From iV curves under nominal operating conditions (see Fig. 13c), the lowest performance is obtained with Cluster1 (lowest OCV).

| | **Cluster1** | **Cluster2** | **Cluster3** | **Cluster4** | **Cluster5** | **Cluster6** | **Cluster7** | **Cluster8** |
|---|---|---|---|---|---|---|---|---|
| Average Cluster Voltage (V) @ OCV | **1.212** | **1.228** | **1.228** | **1.226** | **1.229** | **1.224** | **1.223** | **1.222** |

Table 4. OCV measurements on the 8 clusters of the Stackbox. Each cluster is composed of 4 cells (conditions: 750°C, $H_2/N_2$=3.6/2.4 NmL/min/cm², air=66.7 NmL/min/cm²).

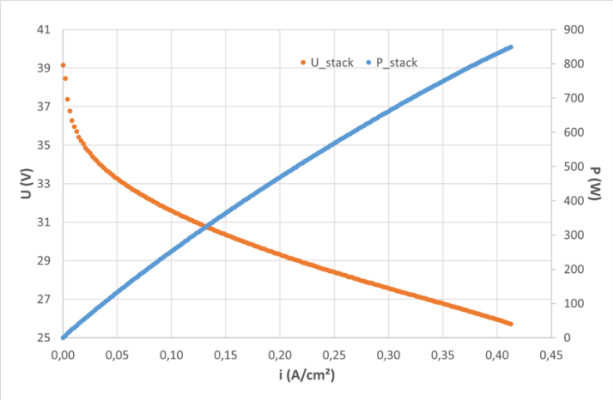


(a)

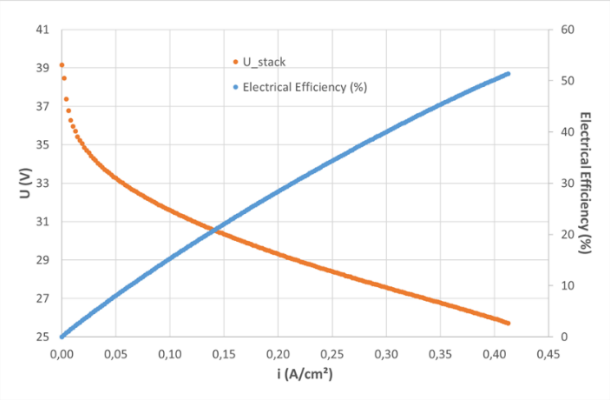


(b)

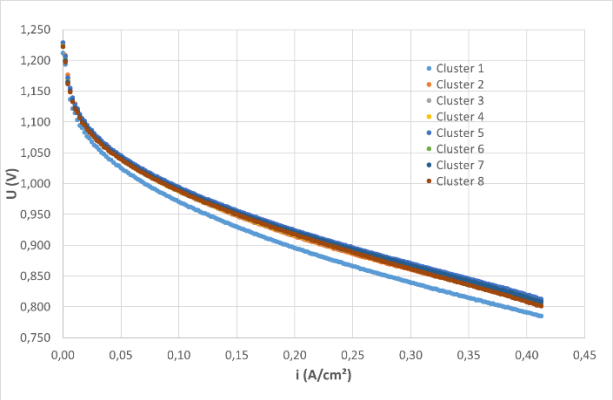


(c)

Fig. 13. Performance achieved on SOLIDpower 32-cells Stackbox at T_Air_Outlet=720°C, in nominal operating conditions: $H_2/N_2$=3.6/2.4 NmL/min/cm², air=66.7 NmL/min/cm²). (a) Stack voltage and Stack Power during i-V characterization, (b) Electrical efficiency during i-V characterization and (c) Voltage of the 8 clusters during i-V characterization.

Figure 14 shows what has been achieved so far under polarization of the Stackbox. First, more than 170 h in nominal operating conditions and i=33 A (FU=0.8), then by applying the fuel starvation protocol, i.e. FU is increased from 0.8 to 0.875 by decreasing $H_2/N_2$ flowrate while current is kept constant at 33 A (summarized in Table 5). EIS/PRBS excitations are implemented by IJS every 6 h at FU=0.8 and at least every 3 h during steps of 24 h at higher FU. PRBS excitation presents the advantage to be faster than sine excitation in these testing conditions. The objective is to see if we are able to detect the signature of fuel starvation at the cluster level despite the averaging.

| Pt. # | Current | Cathode air flow | Cathode air in temp. | Anode N2 flow | Anode N2 flow | Anode H2 flow | Anode H2 flow | FU | AU |
|---|---|---|---|---|---|---|---|---|---|
| | A | NLPM | °C | NLPM | NLPH | NLPM | NLPH | - | - |
| | I | N_air | Tair | N_N2 | N_N2 | N_H2 | N_H2 | | |
| 0 | 33 | 170 | 750 | 6,1 | 366 | 9,20 | 552 | 0,800 | 0,103 |
| 1 | 33 | 170 | 750 | 5,9 | 355 | 8,92 | 535 | 0,825 | 0,103 |
| 2 | 33 | 170 | 750 | 5,7 | 345 | 8,66 | 520 | 0,850 | 0,103 |
| 3 | 33 | 170 | 750 | 5,6 | 335 | 8,41 | 505 | 0,875 | 0,103 |
| 0 | 33 | 170 | 750 | 6,1 | 366 | 9,20 | 552 | 0,800 | 0,103 |

Table 5. Fuel starvation protocol: FU is increased from 0.8 to 0.875 by decreasing $H_2/N_2$ flowrate while current is kept constant at 33 A.

Cluster voltage measurements are relatively close during the first 170 h at FU=0.8 even if fluctuations can be seen due to probably thermal stabilization of the stackbox. When FU is increased to 0.825, 0.85 and finally 0.875, all cluster voltages are gathering. It seems that only at FU=0.875, we can detect some distortion of the signal when EIS/PRBS excitation is superimposed, especially on clusters 3 and 4. It means that we are probably in the non-linear part of the i-V curve and we will get higher THD index. A complete data analysis is needed to confirm this trend.

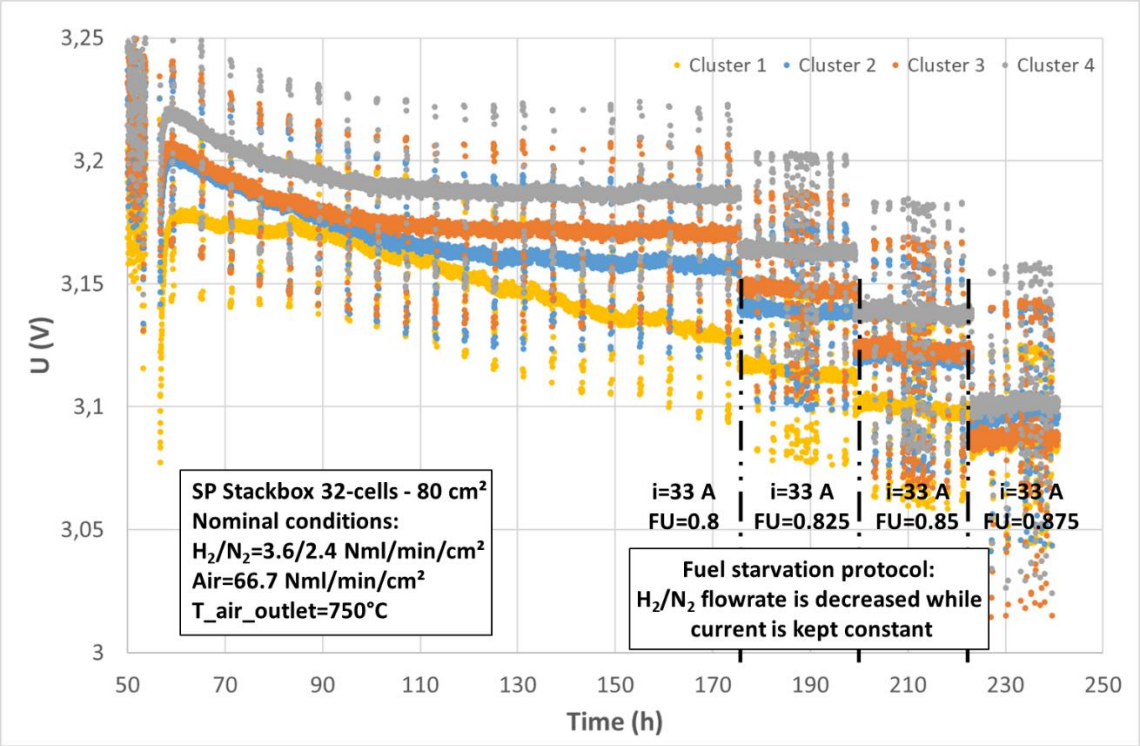


Fig. 14. First part of the fuel starvation protocol on SOLIDpower 32-cells Stackbox. $H_2/N_2$ flowrate is decreased while current is kept constant at 33 A. T_Air_Outlet=750°C.
EIS/PRBS excitations are implemented by IJS every 6 h at FU=0.8 and at least every 3 h during steps of 24 h at higher FU. Note: only 4 clusters are represented here, the 4 others having a similar response.

### 4.2.2. Conclusions on EIS/THD techniques as a detection tool

Test on a 6 cell SS with a sealing defect confirms that a gap located close to the outlet of the stack cannot be easily detected from OCV nor IV characterizations. A specific protocol based on OCV measurements at different air and fuel flowrates seems to give meaningful results.
On the 32-cells Stackbox, PRBS and sine excitations are recorded properly and automatically every 3 h during the fuel starvation protocol where FU is increased from 0.8 to 0.875. A detailed analysis is needed to extract useful information and metrics from these data and to see if we are able to detect the signature of fuel starvation at the cluster level despite the averaging effect.

## 5. Joint tests performed at EPFL in collaboration with AVL

### 5.1. Test setup

The tests set-up consisted of the EPFL stack tester Fig. 15 and the AVL e-Gen Spectrolyzer Fig. 16.

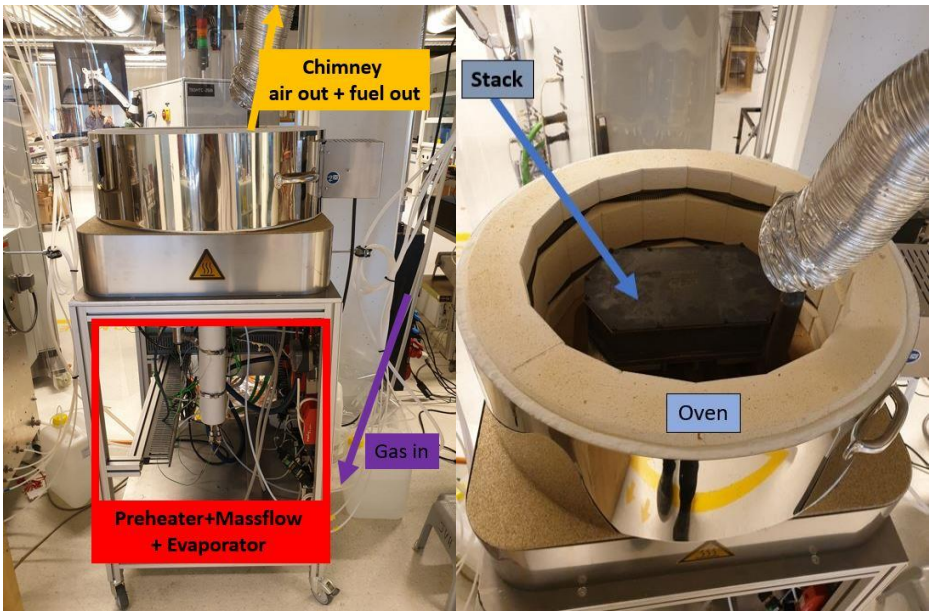


Fig. 15: EPFL SOFC test rig for short stacks. On the left a 6 cell SolidPower short stack inside the furnace.

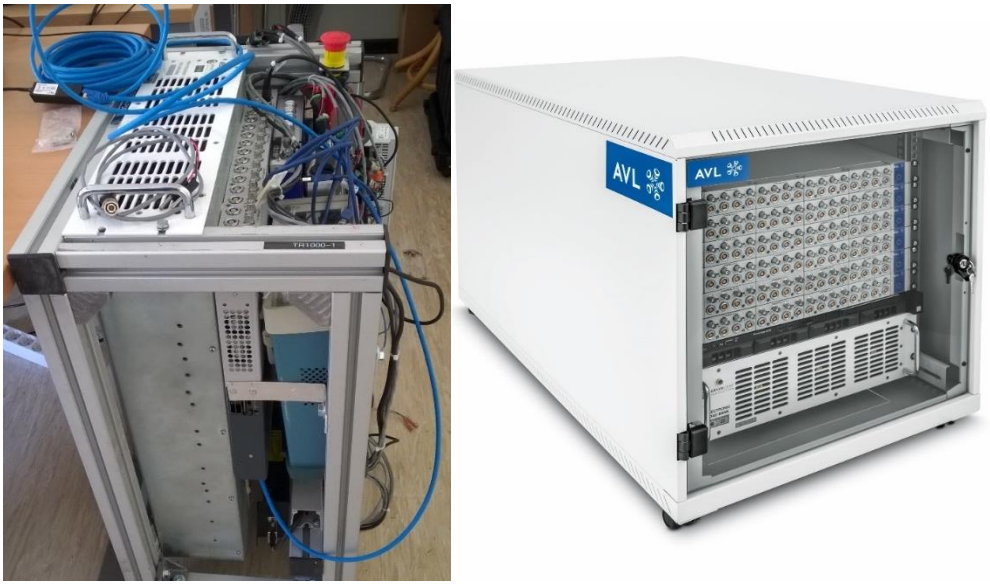


Fig. 16: Two versions of the e-Gen Spectrolyzer, on the left version 1 with one X-Ion base unit (used during the test campaign at EPFL) and on the right version 2 in a commercial 19”-rack (fully equipped with 6 cascaded X-ION and 64 channels, max is 196 channels in parallel).

The e-Gen Spectrolyzer is an assembly that is constituted of two main components: a perturbation unit and data acquisition HW (DAQ / digitizer), the complete topology is displayed in Fig. 17.

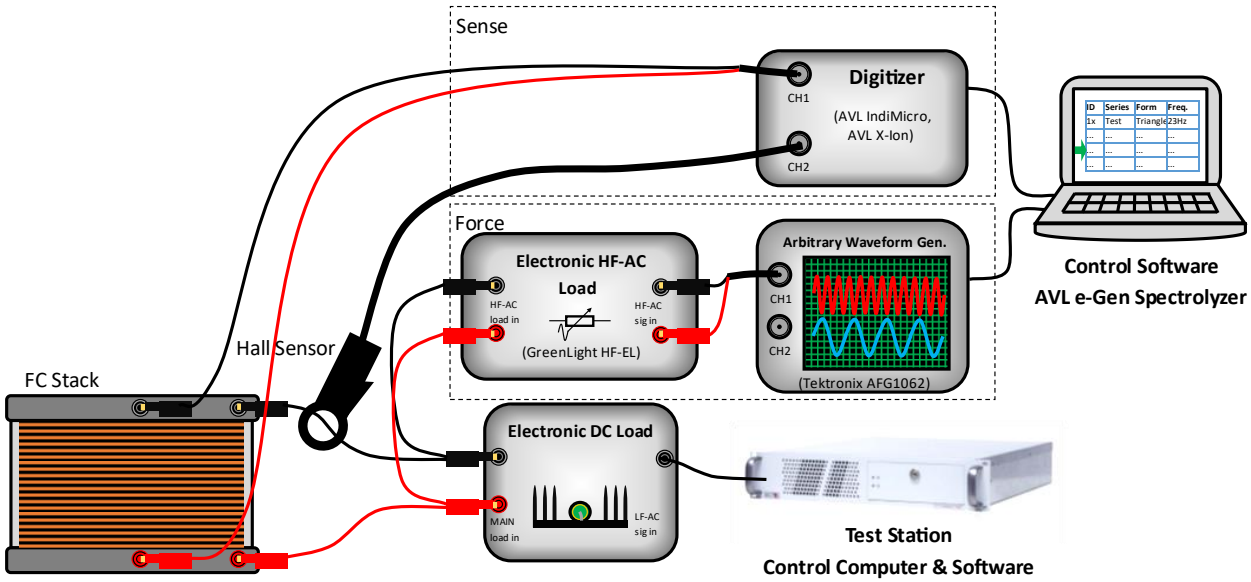


Fig. 17: e-Gen Spectrolyzer configuration at EPFL. Sampling rate of the digitizer AVL X-ION up to 2.0 MHz on multiple channels in parallel. Perturbation unit is a Greenlight Innovation load bank with a dynamic of up to 20 kHz and a max amplitude of 8.0 A.

The digitizer consists of the base unit AVL X-ION and multiple front-end modules of type "e-POWER E4H2.1", each module can record four channels. In the setup at the EPFL 4 of these modules had been installed. The current sensor is a so called Zero-Flux or No-Flux sensor; the advantages are high precision, hardly any hysteresis and a bandwidth up to 150.0 kHz, the sensor has an voltage output of -10 to +10V.


Fig. 18: X-ION Base unit, equipped with different front-end modules (FEM / X-FEM). On the right an e-Power X-FEM with 4 channels. Resolution 18 bit. Voltage range +/- 60 V. Measurement bandwidth 2 MHz.

The specific feature of this unique spectroscopy device is, - beside the access to time domain raw data (needed for the PRBS excitation method from the partner IJS) and the option two measure in parallel all cells -, its AWG[1]-functionality. All signal shapes can be imposed, like non-sinusoidal periodic wavelets or multifrequency excitation or PRBS-patterns. Upfront the testing duty at EPFL the SW of the e-Gen Spectrolyzer had been adopted and experiences during the testing resulted in further improvements of the SW.

[1] AWG: Arbitrary Wavelet Generation.

**Data Quality of e-Gen Spectrolyzer**

The data quality of three different DAQ-systems have been compared by the partner IJS, the three systems are the MDLT[2] by Bitron, the initial set-up used by IJS at CEA (DEWESoft-HW combined with a standard HALL-sensor) and the e-Gen Spectrolyzer (combined with a zero-flux sensor), see Fig. 19. Regarding the current signals, it is quite clear that the measurements from MDLT-board, where the current was measured via a shunt resistor exhibit the lowest signal-to-noise ratio. These signals are followed by the ones recorded with the IJS-ver1-HW (DEWEsoft digitizer combined with a standard Hall probe) at CEA in 2018. Finally, there is AVL data with Zero-Flux current sensor used at EPFL in 2018/2019 that have the highest quality.

A comparison of the voltage measurement is difficult, because the three systems have been operated on different systems: a) MDLT attached to micro-CHP system from SolidPower, b) IJS vers1-HW operated in the CEA-lab, c) e-Gen Spectrolyzer at an EPFL short stack tester.

To conclude, regarding the current measurement, there is undoubtedly a clear choice that Zero-Flux data are the best. Regarding the voltage the situation is quite difficult due to the influence of the test bed.

a) MDLT with a shunt resistor:

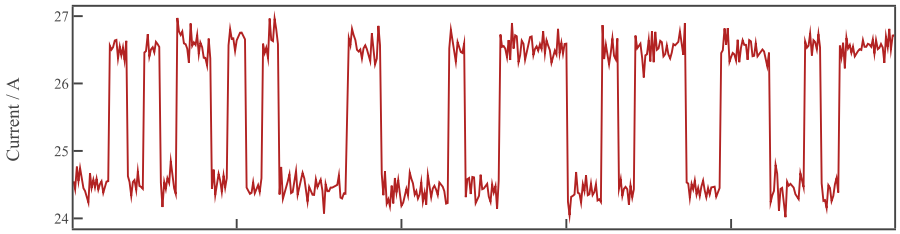


b) IJS vers1-HW with standard HALL sensor:

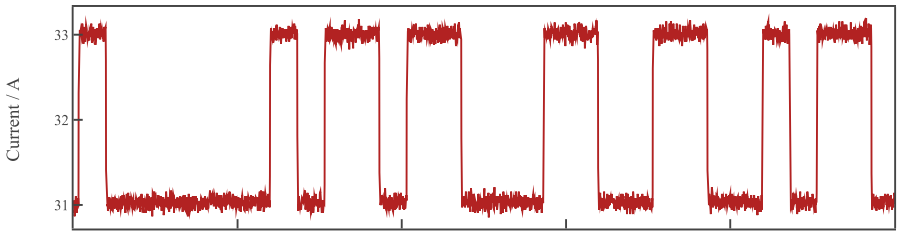


c) e-Gen Spectrolyzer with Zero-Flux sensor:

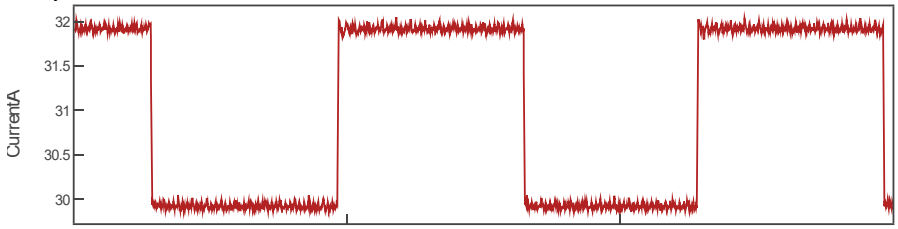


Fig. 19: Comparison of three DAQ-devices: a) MDLT (Monitoring, Diagnostic and Lifetime Tool), b) IJS vers1-HW, c) AVL e-Gen Spectrolyzer.

## 5.2. Description of the tests

The tests were performed on 2 short stacks from Solid Power (UUT1 & UUT4) with 6 cells and an open surface area of 80.0 mm². First tests were taken on UUT4 (sealing issue), the 2nd on UUT1 without defects. To enable a comparison both where tested in four equal fuel utilisations from 70% up to 85%. Because of the defect of UUT4, the test conditions were chosen less severe. The upper FU was 85% for UUT4 instead of 90% for UUT1. Also, the other conditions like test station,

[2] Monitoring, Diagnostic and Lifetime Tool

temperature and fuel composition had been the same. Beside the validation of the THDA methodology on SOFC another objective had been to investigate, if the sealing issue in UUT4 are visible. Different methods have been used: EIS, IMD, THDA, PRBS.

UUT4:

First various EIS spectra had been recorded, mainly to check for possible hardware or software problems. The testing hardware was calibrated. The test protocol included testing three different test regimes:

**1) Variation of fuel utilization:**

Mainly THD (Total harmonic distortion) and EIS tests were performed at 5 different fuel utilizations 65, 70, 75, 80, 85 %. The corresponding H2 and N2 flows can be seen in Table 6.

| Fuel utilization (%) | H2 (NL/min) | N2 (NL/min) |
|---|---|---|
| 65 | 1.926 | 1.284 |
| 70 | 1.791 | 1.194 |
| 75 | 1.672 | 1.114 |
| 80 | 1.567 | 1.045 |
| 85 | 1.475 | 0.983 |

Table 6: Fuel utilization and corresponding H2/N2 flows on UUT4, H2/N2 ratio of 60%/40%.

**2) Constant current mode**

The current was kept constant at 30A DC with a fuel utilization of 80% which equals 1.567 NL/min H2 and 1.045 NL/min N2.

**3) Constant power mode**

The power drawn (P = U*I) is kept constant over the test duration. The used fuel utilization was 80% which equals 1.567 NL/min H2 and 1.045 NL/min N2.

**UUT1**

The test protocol for UUT1 was designed in a similar way to UUT4. The goal was to perform a 1200-hour fulltime test to include aging behaviour of the stack. The hardware setup was the same as for UUT4. Tests performed were variation of fuel utilization, constant current mode and carbon deposition tests.

**1) Variation of fuel utilization:**

Mainly THD (Total harmonic distortion) and EIS tests were performed at 5 different fuel utilizations 70, 75, 80, 85, 90 %. The corresponding H2 and N2 flows can be seen in Table 7.

| Fuel utilization (%) | H2 (NL/min) | N2 (NL/min) |
|---|---|---|
| 70 | 1.791 | 1.194 |
| 75 | 1.672 | 1.114 |
| 80 | 1.567 | 1.045 |
| 85 | 1.475 | 0.983 |
| 90 | 1.393 | 0.929 |

Table 7: Fuel utilization and corresponding H2/N2 flows on UUT1, H2/N2 ratio of 60%/40%.

**2) Constant current mode**

The current was kept constant at 30A DC with a fuel utilization of 80% which equals 1.567 NL/min H2 and 1.045 NL/min N2.

**3) Carbon deposition tests**

The goal of the tests was to detect carbon deposition on the stack, when using CH4 and H2O steam instead of H2 and N2. The set steam to carbon ratio was at the beginning 1.0 and had been reduced 0.5. FU was constant at 80%. This approach was motivated by the findings of the partner DTU that no carbon was formed at 30 A and S/C = 0.5. To increase the probability of carbon formation the test plan was to decrease the DC-bias in steps (duration each step 24h):
S/C: 1.0; a) I: 30 A,
S/C: 0.5; b) I: 30 A, c) 20 A, d) 15 A, e) 10 A, e) 5 A

## 5.3. Faults/failure implemented

**UUT4**

Beside the constant current mode also a constant power mode had been added to the test regime as described in the standard test protocol provided by the partner DTU. In combination with a missing voltage threshold to limit the DC-current a problem occurred while testing under constant power mode. Due to constant power mode the test station kept increasing the current to compensate for the decrease of voltage. As the test station had no limits implemented for maximum current drawn it peaked out at 102.8 A, as can be seen in Fig. 20. This destroyed the stack. Especially RU 3 was damaged badly, which made further testing on UUT4 impossible.

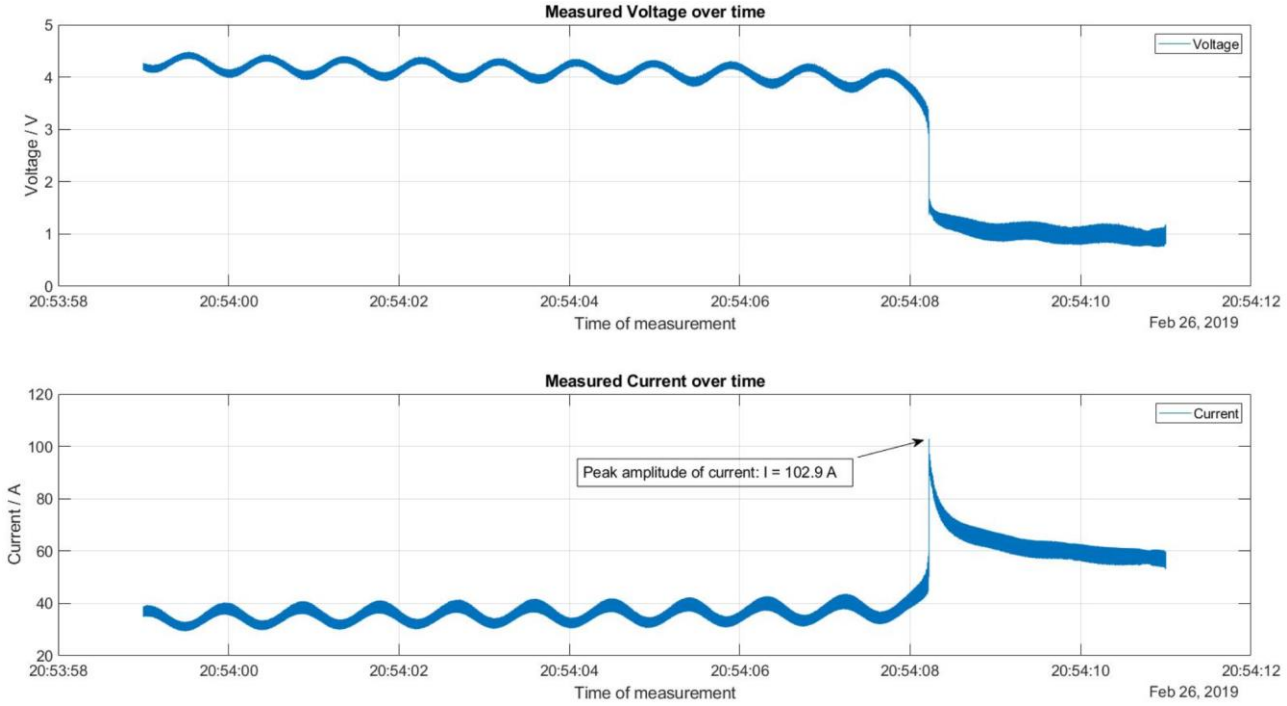


Fig. 20: Incident that led to the ruin of UUT4. We can observe a slight decrease of voltage which let to the test station rapidly increasing the current.

**UUT1**

Problems occurred while performing carbon deposition tests, which were the last tests that should be done. The set steam to carbon ration was too high. The carbon deposition was too fast and damaged the stack. The following tests were readjusted. Especially RU6 was damaged and couldn't further perform the set current of 30A. The current was lowered to 15A for the last tests which were performed on H2 and N2.

## 5.4. Results for EIS

### Variation of Excitation Current

To figure out which excitation current is suitable to measure impedance spectra the current amplitude had been varied in four steps form 0.5 up to 2.0 A, which is equivalent to a current density range from 6.25 to 25.0 mA/cm². To fulfil the requirement of linearity between perturbation and response, impedance values for one frequency must be the same for the excitation range that is inside the linear domain. As shown in Fig. 21 the impedances for the same frequencies show a sensitivity on the excitation amplitude, which indicates a non-linear behaviour of the voltage response. Therefore, the lowest imposed amplitude of 0.5 A is the most appropriate choice in this range. This is an unexpected result, as it was anticipated that 1.0 A should be feasible at a current DC BIAS of 30.0 A.

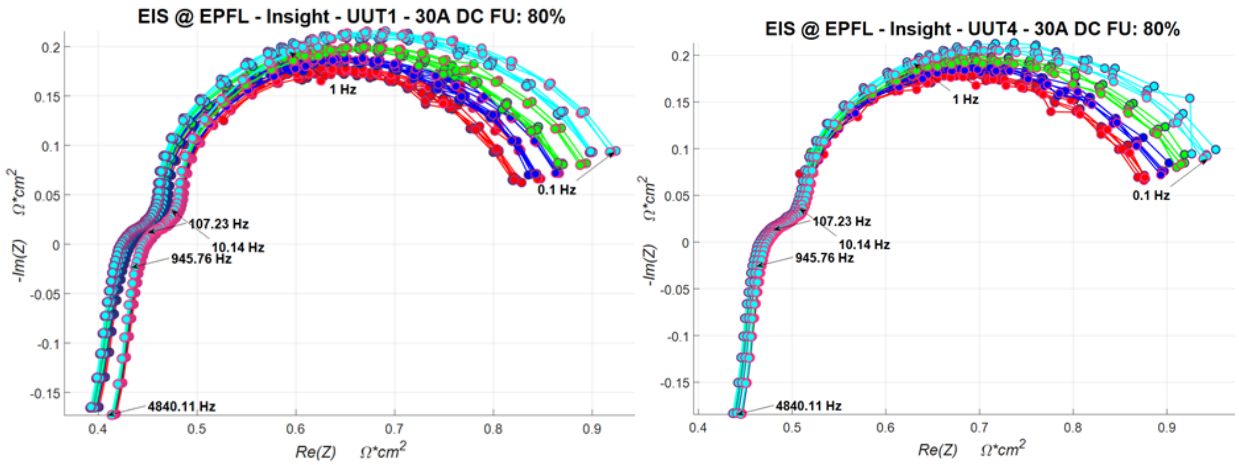


Fig. 21: EIS on UUT1 (left) and UUT2 (right) with the same fuel utilization (FU) and the same DC current BIAS of 30 A. The different colours represent different amplitudes of excitation currents: red 0.5 A, blue 1.0 A, green: 1.5 A, light blue: 2.0 A.

**UUT4**

EIS tests were performed on UUT4 over a period of 10 days as seen in Fig. 22. There is no significant change in impedance spectra over the test period for either of the 4 tested AC currents.

The difference in impedance between the distinct AC excitation currents at lower frequencies indicates a nonlinear behaviour of the stack at set stoichiometry. This is rather odd because the used excitation current was well under 10% of the set DC current of 30A. A possible explanation might be that the extremely low frequencies (0.1 … 1 Hz) over or under supply the stack with hydrogen. As seen in Fig. 22. The impedance spectra get more similar the higher the frequency of the imposed current.

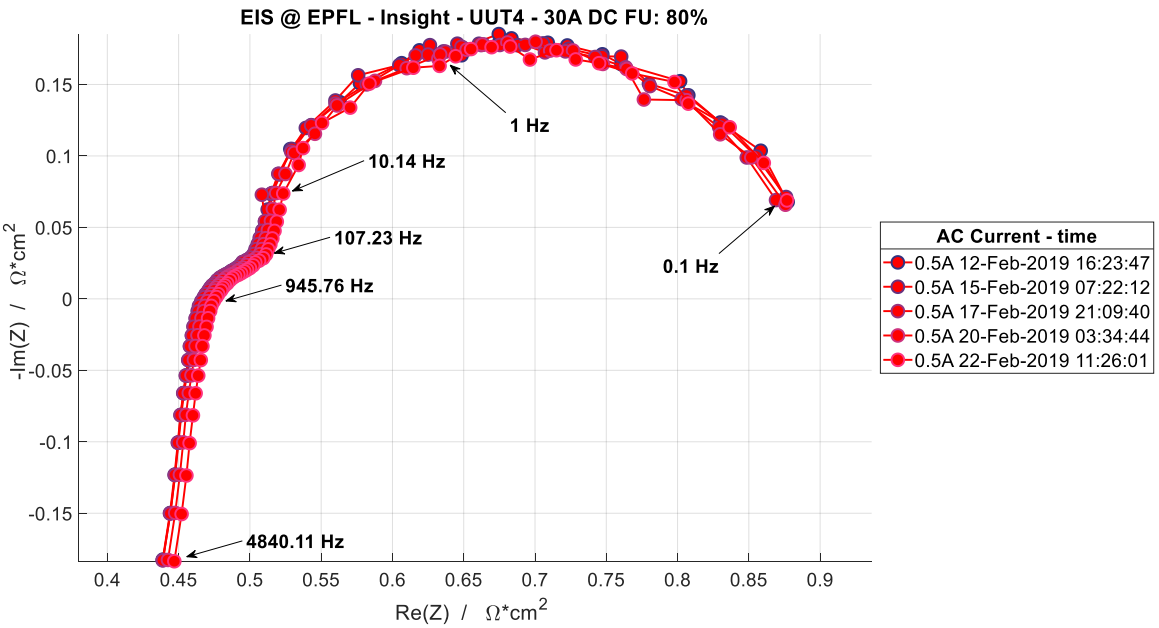


Fig. 22: EIS tests performed on UUT4. Cell area: 80 cm².

As seen in Fig. 23. There is no significant change in impedance spectra over the test period. This can be explained by the shorter test period due to the incident that happened while testing in constant power mode.

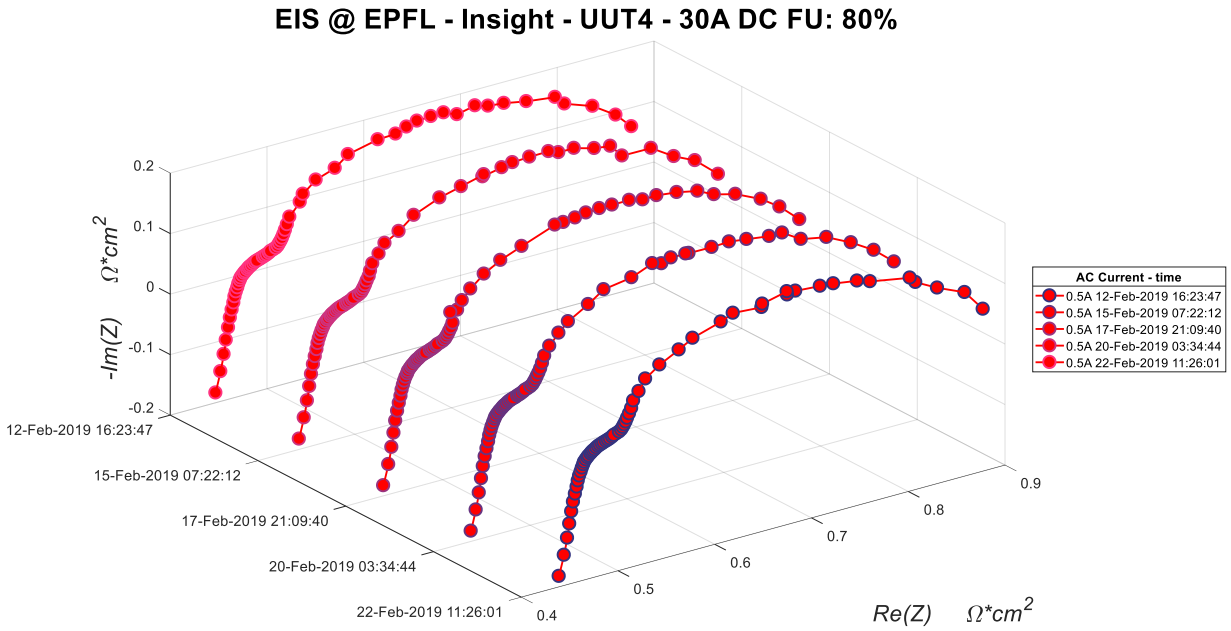


Fig. 23: EIS tests performed on UUT4, cell area: 80 cm².

**UUT1**

The EIS tests on UUT1 were performed from 29th of March 2019 till the 6th of May 2019. In contrast to UUT4 a change in impedance can be noticed over the test period. The data reveals that the change in impedance happened around 27th of April. Not only the electrolyte suffered (loss of ion-conductivity), but also the electrodes suffered, the radius low frequency arc increased that much that the two arcs cross each other. The test station data was analysed together with the EPFL to track down

the root cause for this sudden degradation, but no fluctuation of media flows or temperatures could be observed during the period of rapid degradation.

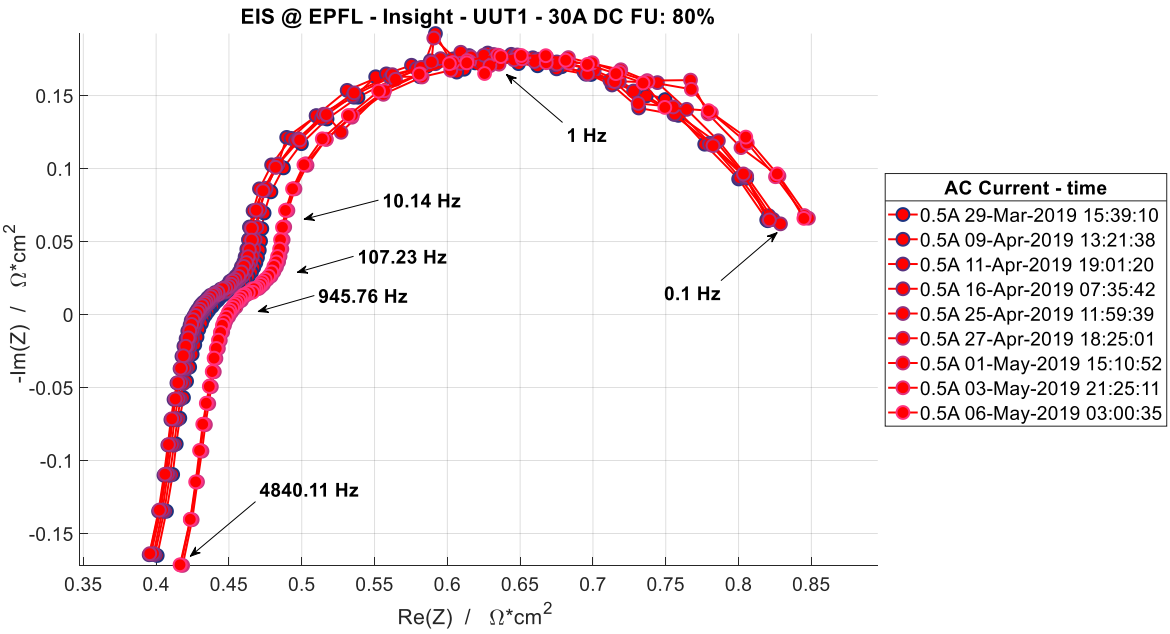


Fig. 24: EIS tests performed on UUT1. The difference in impedance is seen at higher frequencies. Cell area: 80 cm²

To have a more detailed view the two groups of EIS ("before" and "after") have been plotted in Fig. **25** in separate graphs. It becomes clear that in the group "after" no further degradation is noticeable.

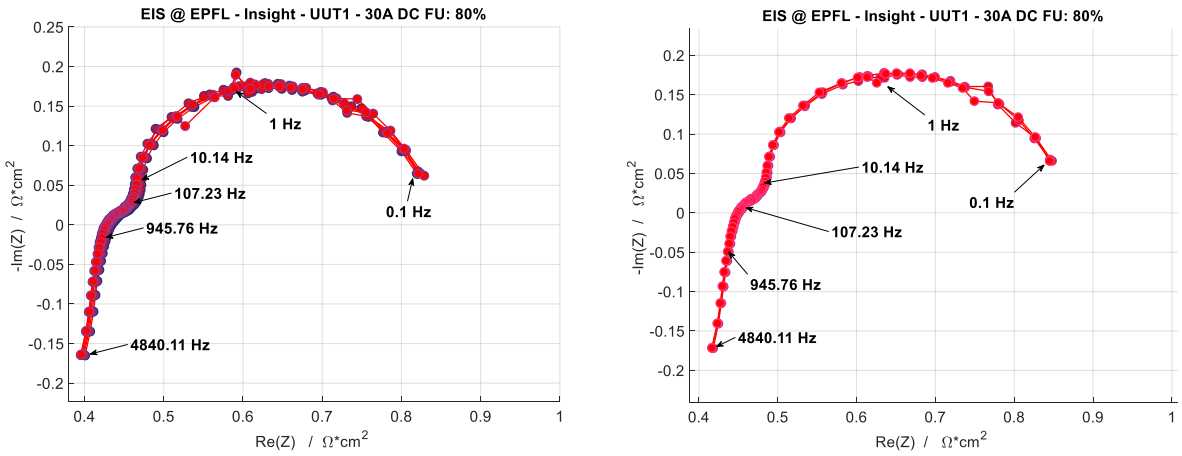


Fig. 25: Before (left) and after (right) the 27th of April. The stack degraded in a short period of time.

The change in H2 and N2 flows of the stack can be seen in Fig. 26.

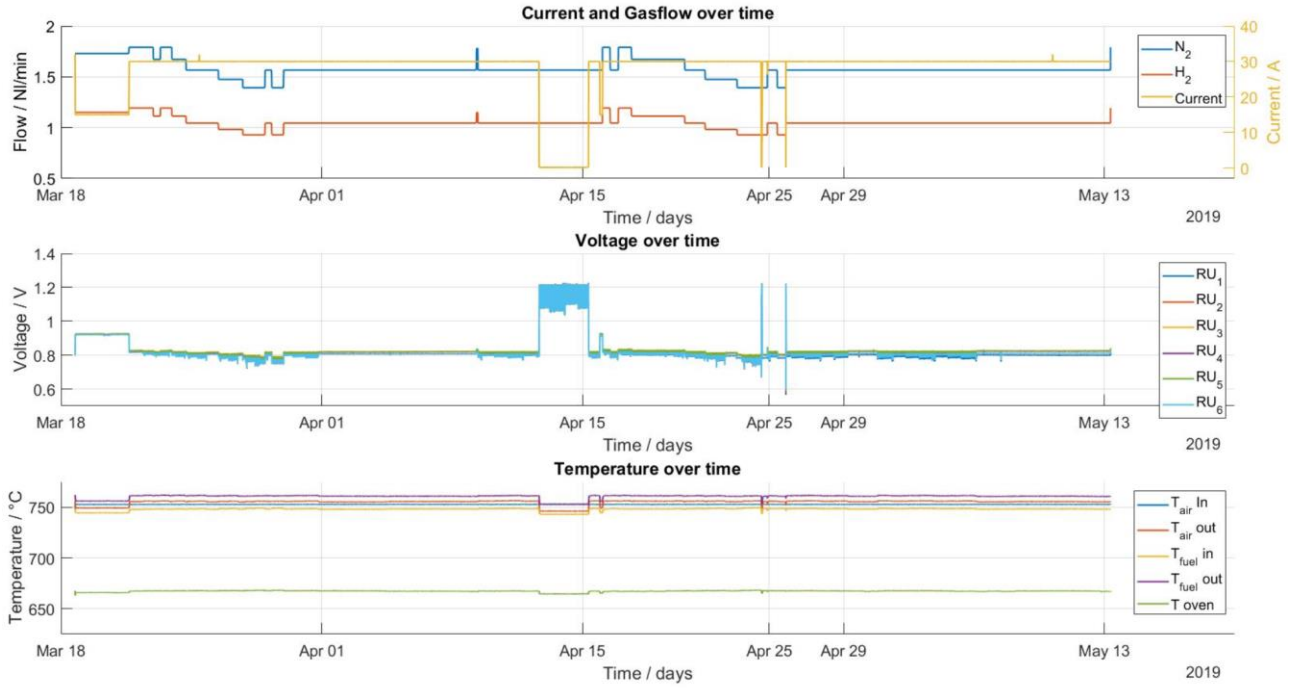


Fig. 26: Current, gas-flow, cell-voltages and temperature of the stack over whole test duration.

## 5.5. Results for THDA

Total harmonic distortion analysis has been proven to be a good tool to detect current fuel utilization, as can be seen in Fig. 27. The index quality (monotony and steadiness) correlates with the imposed frequency and tends to fall off the higher the imposed frequency is. As UUT 4 includes a repeating unit with a manipulated sealing THDA plots are show for both UUT to investigate if a difference of THD is detectable on RU-level (see Fig. **28** / Fig. **29**). As the manipulated RU is RU4 the THD for this RU might show a deviating course of curve. If the numbering was flipped in the labelling of channels RU4 nominal might be in Fig. **29** the curve with the label RU2. And as a matter of fact, the courses of curves in Fig. **29** shows nonuniform character. The line with label RU2 shows an unexpected maximum at a mild FU of 70%. Due to the leaking sealing it is expected that the THD for the manipulated RU has a steeper course toward higher FU, but for RU2 it is the opposite. The conclusion is: The reason for a deviating THD characteristics of RU2 in Fig. **29** is not related to a sealing issue.

**UUT1**

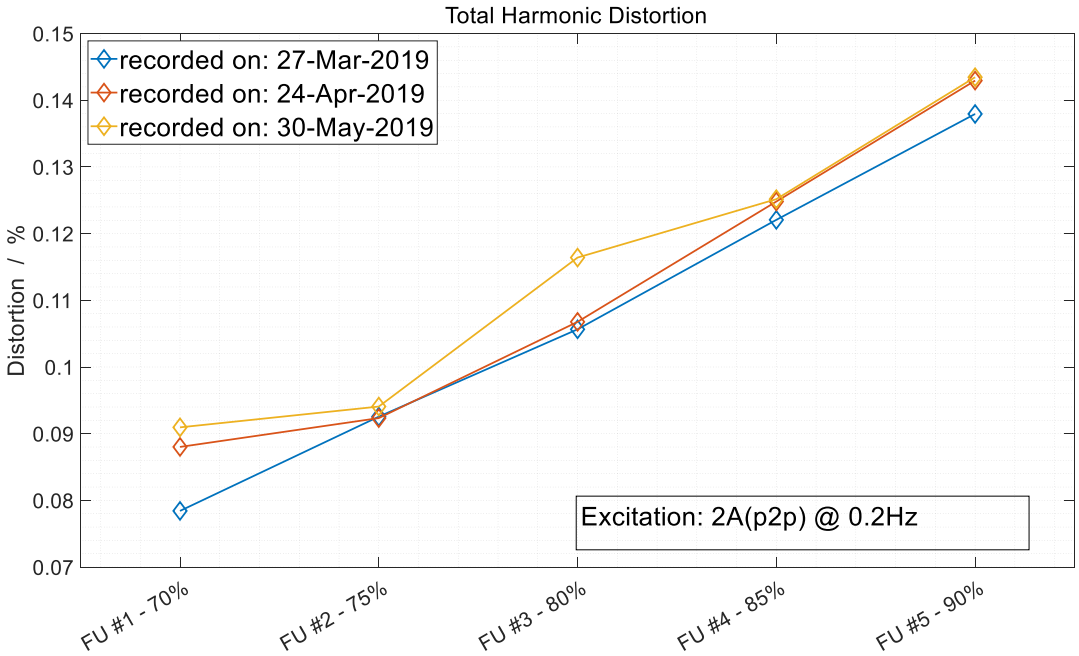


Fig. 27: THD over fuel utilization for UUT1over whole test duration.

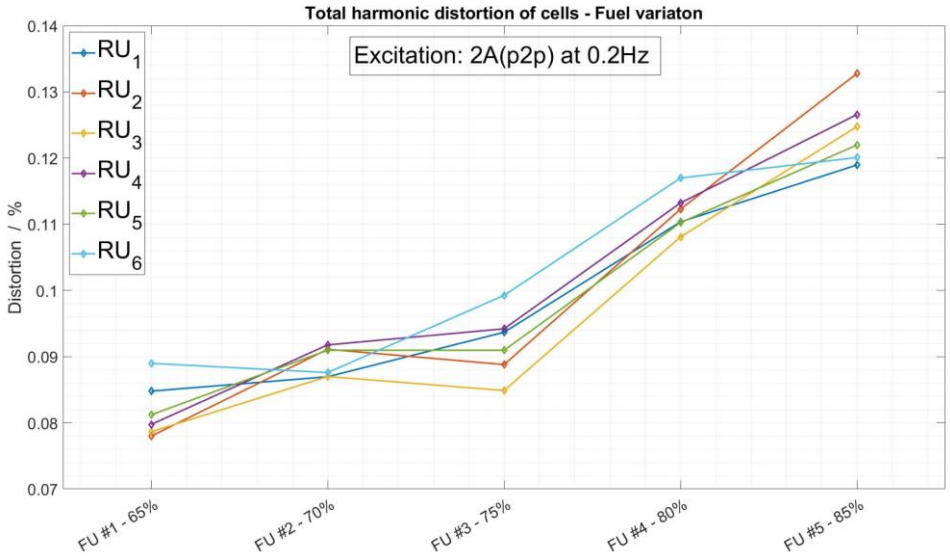


Fig. 28: THD over fuel utilization for UUT1 on repeating unit level.

**UUT4**

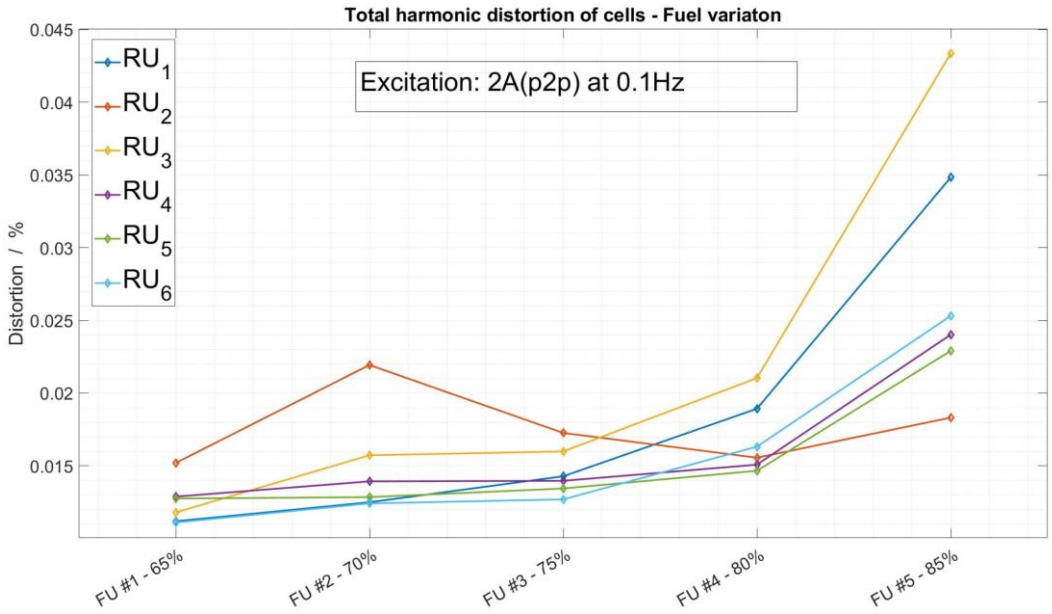


Fig. 29: THD over fuel utilization for UUT4 on repeating unit level.

### 5.6. Conclusions on EIS/THDA Techniques as a Detection Tool

The e-Gen Spectrolyzer was capable to record EIS-data in good quality, even at a low excitation amplitude of 0.5 A (0.00625). At the same fuel, temperature and current density EIS is suitable to detect electrode as well as electrolyte degradation on stack level.
The THDA method is sensitive to higher FU even far away from the critical region above FU = 75%, the method is therefore a suitable indicator to enhance system reliability combined with higher efficiency, for more details please refer to D3.7.

## 6. Conclusions

The aim of this document is to present the results of the tests performed in WP2 during the second reporting period. Tests have been performed at DTU, EPFL and CEA according to test protocols and specifications defined in D2.1 with a focus on 3 faults/failure: fuel starvation, carbon deposition and gas leakage. EIS associated to DRT analysis, THD and PRBS measurements as well as conventional signals have been considered and their potential as detection and diagnostic tools has been evaluated. AVL and IJS have installed their specific devices respectively at EPFL and CEA to be used for measurements during the tests.

For the testing campaign presented in the present report, carbon deposition and gas leakage are considered for short stack testing campaign.
Finally, a 32-cell stackbox has been tested, with the fuel starvation protocol.

*Carbon deposition:*
Two different experiments were conducted and EIS on the single RU and stack level were implemented to detect flawed operating conditions, which could cause detrimental failure by locally introduced carbon formation. Generally, it could be observed that in both simulated cases, these changes led to increase in cell voltage which seems to be a good metric extractable solely from the stack voltage. Furthermore, the complimentary use of EIS measurements/metrics on stack level allow detection of the condition changes. In the first case (=SC ratio reduction), an increase of high frequency area specific resistance in parallel with a decrease of the low frequency arc indicates possible critical conditions. In the second case, again an increase of the high frequency circle, together

with an increase of the low frequency arc can be used as a detection metric for unsafe conditions. Yet both simulated failures, did not give any indication of a final detrimental failure occurring inside the stack.

*Gas leakage*

A gap sealing close to the outlet of the stack cannot be easily detected from OCV nor IV characterizations. A specific protocol based on OCV measurements at different air and fuel flowrates seems to give meaningful results.

The defect “gap in the sealing close to the stack inlet” can be more easily detected than a gap located close to the outlet of the stack. It can most clearly be observed in the OCV. At the RU level its signature is related to the increase in steam content, which results in a reduction of the polarization resistance as measured by EIS. DRT analysis reveals that it is the gas conversion peak (P2) that is reduced, whereas peak P3, which is attributed to gas diffusion in the porous anode structure, is shifted towards higher frequencies. However, at the cluster level, this signature cannot be detected anymore due to averaging with defect-free RUs.

*Stackbox test*

On the 32-cells Stackbox, PRBS and sine excitations are recorded properly and automatically every 3 h during the fuel starvation protocol where FU is increased from 0.8 to 0.875. A detailed analysis is needed to extract useful information and metrics from these data and to see if we are able to detect the signature of fuel starvation at the cluster level despite the averaging effect.

*Use of classical signals*

Classical signals remain a useful tool to see a deviation of a stack/system from its standard operating conditions. It was particularly useful for the case of a leakage, in association with some specific deviation trials as compared to the nominal operating conditions to highlight the issue.

*EIS*

EIS was found to be an adequate technique to identify the carbon deposition fault, at stack level.

On the contrary, for gas leakage, it was found to be efficient at the RU scale, and DRT analysis further allowed to identify the frequency signature of the defect. However, on the clusters level (6-cell short stack), the signature of the defect was unfortunately lost through averaging.

*PRBS*

EIS diagrams extracted from PRBS excitation are well superimposed to those obtained from sines excitation, meaning that PRBS is a valuable technique in order to obtain faster EIS results that do not disturb too long the stack/system from its setpoint during real operation.

*THD*

The THDA method is sensitive to higher FU even far away from the critical region above FU = 75%, the method is therefore a suitable indicator to enhance system reliability combined with higher efficiency.